

New Aspects of Spin Diffusion and Cross Relaxation in Solid-State NMR

A. Müller, H. Zimmermann, and U. Haeberlen

Max-Planck-Institut für Medizinische Forschung, Arbeitsgruppe Moleküllkristalle, Jahnstraße 29, 69120 Heidelberg, Germany

Received October 11, 1996; revised January 15, 1997

Theoretical models for motionally driven spin diffusion are compared and applied to spins $S = \frac{1}{2}$ and $S = 1$. Their predictions are quantitatively corroborated by experiments on a single crystal of deuterated biphenyl. In this system, a molecular flip process drives spin diffusion and makes it strongly temperature dependent. In the second part, it is shown how spin diffusion of quadrupolar order degenerates into cross relaxation. A single crystal of partially deuterated durene provides a clear-cut example of cross relaxation in a dipolar coupled pair of spins $S = 1$. This observation explains why, in solids, the relaxation time of quadrupolar order, T_{1Q} , is often much shorter than T_1 . © 1997 Academic Press

INTRODUCTION

In the past decade, measurements of molecular dynamics by 1D or 2D exchange NMR have progressed to longer and longer correlation times (1), and they have reached the point where spin diffusion becomes a major concern. This is due to the long understood fact that spin diffusion and chemical exchange lead to the same features in 2D and other exchange experiments (2). There is therefore a need to discriminate between these two processes that are of very different nature. We have recently shown by experiments on a deuterated single crystal of biphenyl that spin diffusion may strongly depend on the temperature of the sample (3). As a consequence, the measurement of the temperature dependence of, say, 2D spectra provides no reliable criterion to distinguish spin diffusion from thermally activated chemical exchange. In the discussion of those experiments, we mostly relied on analogies with proton-driven spin diffusion (2) and intuitive arguments. In a recent review article on spin diffusion (4), Meier discussed, using a two-spin model, the possibility of motionally driven spin diffusion without, however, providing experimental evidence. In this article, we return to his two-spin model and compare it with a more realistic three-spin model to show that the former is fully satisfactory. We then apply it to deuterons, i.e., spins $S = 1$, and justify our intuitive reasoning in (3). Experiments on a single crystal of deuterated biphenyl (3) have meanwhile been extended to lower temperatures and now also include spin diffusion

of quadrupolar order. All measured data nicely fit the theoretical predictions.

When quadrupolar order instead of Zeeman order is stored during the mixing time of an exchange experiment, one often observes that its relaxation time T_{1Q} is much shorter than T_1 . This phenomenon, which contradicts the common understanding of these relaxation times (5), has not been adequately dealt with in the literature. We will show that T_{1Q} can be dominated by a cross-relaxation process which appears as a degenerate case of spin diffusion. The time constant of this process is in the range of seconds to many tens of seconds for deuterons. This is the same range as that of spin diffusion. Therefore, it is only observed when T_1 substantially exceeds this range. We present measurements on a single crystal of partially deuterated durene that provide conspicuous evidence of this phenomenon.

TEMPERATURE DEPENDENCE OF SPIN DIFFUSION

Basic Theory of Motionally Driven Spin Diffusion

Spins $S = \frac{1}{2}$. We first consider a system of two spins $S = \frac{1}{2}$ that are chemically shifted and dipolar coupled. Its Hamiltonian is given by

$$H = \omega_1 \mathbf{S}_{1z} + \omega_2 \mathbf{S}_{2z} + D \{ 2\mathbf{S}_{1z}\mathbf{S}_{2z} - \frac{1}{2}(\mathbf{S}_{1+}\mathbf{S}_{2-} + \mathbf{S}_{1-}\mathbf{S}_{2+}) \} \quad [1]$$

where ω_1 , ω_2 and D are the two chemical shifts and the strength of the dipolar coupling. To calculate the spin diffusion rate in this system, we start from a state of pure polarization,

$$\begin{aligned} \rho(0) &= x\mathbf{S}_{1z} + y\mathbf{S}_{2z} \\ &= \frac{x+y}{2} (\mathbf{S}_{1z} + \mathbf{S}_{2z}) + \frac{x-y}{2} (\mathbf{S}_{1z} - \mathbf{S}_{2z}) \quad [2] \end{aligned}$$

with arbitrary amounts x and y of single-spin polarization. Because $\mathbf{S}_{1z} + \mathbf{S}_{2z}$ commutes with H , only the component

$\mathbf{S}_{1z} - \mathbf{S}_{2z}$ of the density matrix is affected by the magnetic interaction. Therefore, we can specialize to the case

$$\rho(0) = \mathbf{S}_{1z} - \mathbf{S}_{2z}. \quad [3]$$

The evolution of this density matrix is limited to a three-dimensional subspace of the full Liouville space (4). This subspace is spanned by the basis operators

$$\begin{aligned} \mathbf{O}_1 &= \mathbf{S}_{1z} - \mathbf{S}_{2z}, \\ \mathbf{O}_2 &= \mathbf{S}_{1+}\mathbf{S}_{2-} - \mathbf{S}_{1-}\mathbf{S}_{2+}, \\ \mathbf{O}_3 &= \mathbf{S}_{1+}\mathbf{S}_{2-} + \mathbf{S}_{1-}\mathbf{S}_{2+}. \end{aligned} \quad [4]$$

The density matrix is thus given at any time by $\rho(t) = a_1(t)\mathbf{O}_1 + a_2(t)\mathbf{O}_2 + a_3(t)\mathbf{O}_3$. The Liouville equation

$$\dot{\rho} = -i[H, \rho] \quad [5]$$

in the basis of Eq. [4] transforms to a linear differential equation $\dot{\mathbf{a}} = \mathbf{A}\mathbf{a}$ for the vector $\mathbf{a}(t) = [a_1(t), a_2(t), a_3(t)]$ with the matrix

$$\mathbf{A} = -i \begin{bmatrix} 0 & D & 0 \\ D & 0 & \Delta \\ 0 & \Delta & 0 \end{bmatrix}, \quad [6]$$

where $\Delta = \omega_1 - \omega_2$ is the chemical-shift difference of the two nuclei. The solution of this system of equations shows a characteristic zero-quantum oscillation of the expectation value $\langle \mathbf{S}_1 - \mathbf{S}_2 \rangle$ (4). It will decay only when a broadening effect is added to the two-spin interaction. We first follow Meier (4) in the description of the broadening introduced by a motional process. Let us assume that the resonance frequency of the second nucleus is not constant in time but fluctuates erratically with a rate k between the values ω_2 and ω_2^* . This can happen, for example, by a molecular jump process between two sites with different chemical shifts, a situation depicted in Fig. 1a. It is described in a composite Liouville space (4, 7, 8) representing a coupled spin pair alternating between two states defined by parameters (ω_1, ω_2, D) and $(\omega_1, \omega_2^*, D)$, respectively. (For simplicity, we assume that the dipolar coupling strength D is the same in both states.) In the basis $\mathbf{O}_1, \mathbf{O}_2, \mathbf{O}_3, \mathbf{O}_1^*, \mathbf{O}_2^*, \mathbf{O}_3^*$, where the starred operators apply to the second state, the matrix \mathbf{A} for the linear differential equation is written

$$\mathbf{A} = \begin{bmatrix} -k & -iD & 0 & k & & & \\ -iD & -k & -i\Delta & & k & & \\ 0 & -i\Delta & -k & & & k & \\ k & & & -k & -iD & 0 & \\ & k & & -iD & -k & -i\Delta^* & \\ & & k & 0 & -i\Delta^* & -k & \end{bmatrix}, \quad [7]$$

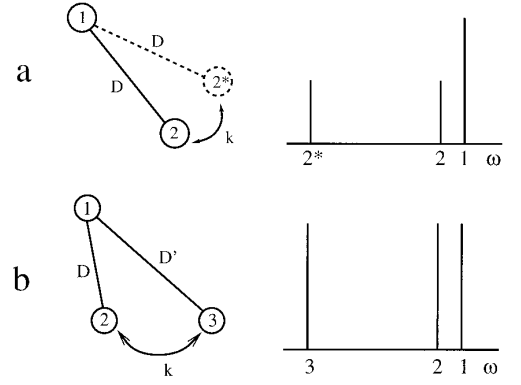


FIG. 1. Two models for motionally driven spin diffusion and their spectra in the slow-motion limit. (a) Two spin $S = \frac{1}{2}$ nuclei with dipolar coupling D and individual chemical shifts. Spin 2 fluctuates at a rate k between two equilibrium positions with chemical shifts ω_2 and ω_2^* . (b) Three nuclei with two different dipolar couplings and individual chemical shifts. Nuclei 2 and 3 exchange at a rate k . The dipolar coupling is disregarded in the representation of the spectra.

where $\Delta^* = \omega_1 - \omega_2^*$. Calculating the spin-diffusion rate in this system means calculating the decay rate of the polarization difference of the average of the two states, i.e., the expectation value $\langle \mathbf{O}_1 + \mathbf{O}_1^* \rangle$. For $D = 0$, $\mathbf{O}_1 + \mathbf{O}_1^*$ is an eigenvector of the system and its eigenvalue λ is zero. If D is small (in a sense we will state below), $\mathbf{O}_1 + \mathbf{O}_1^*$ is still approximately an eigenvector, and we may expand the eigenvalue λ as a power series of D ,

$$\lambda = aD + bD^2 + cD^3 + O(D^4). \quad [8]$$

Insertion of Eq. [8] into the characteristic polynomial of \mathbf{A} , and setting this polynomial to zero, yields the coefficients a , b , and c . The solution found with the help of computer algebra is

$$\lambda = \frac{-k(\Delta^* - \Delta)^2 D^2}{2\Delta^2 \Delta^{*2} + 2(\Delta + \Delta^*)^2 k^2} + O(D^4). \quad [9]$$

For D small, the decay of $\langle \mathbf{O}_1 + \mathbf{O}_1^* \rangle$ is almost single exponential, and $-\lambda$ can therefore be identified with the spin-diffusion rate. Note, however, that D small means $D \ll \Delta$, Δ^* , $(\Delta + \Delta^*)/2$. This means that the dipolar coupling must be small compared to the chemical-shift differences Δ and Δ^* in the slow-motion limit and also small compared to the averaged chemical-shift difference $(\Delta + \Delta^*)/2$, which applies to the fast-motion limit. The spin-diffusion rate found in this way agrees with Meier's results for the slow- and fast-motion limits, $k \ll |\Delta^* - \Delta|$ and $k \gg |\Delta^* - \Delta|$, but in addition covers the whole range of rates k . For an interpretation of Eq. [9], we specialize to the case $\Delta^* \gg \Delta$

$\gg D$. A schematic spectrum for this case is shown in Fig. 1a. In this limit, the spin-diffusion rate is

$$\frac{1}{T_{\text{SD}}} = \frac{1}{2} \frac{D^2 k}{\Delta^2 + k^2}. \quad [10]$$

We conclude that, for slow exchange ($k \ll \Delta$), the spin-diffusion rate is proportional, on the one hand, to the exchange rate k and, on the other, to the inverse square of the smaller of the chemical-shift differences. According to the general theory of spin diffusion (4, 9), the Δ dependence of $1/T_{\text{SD}}$, Eq. [10], reflects a Lorentzian broadening of the zero-quantum ($\Delta M = 0$) transition that exists in the two-spin system with $S = \frac{1}{2}$. The lineshape of this transition is

$$g(\Delta) = \frac{k}{2(\Delta^2 + k^2)}.$$

A molecular motion process in a real solid usually differs from our model in so far as there are not two states for one nucleus but two nuclei exchanging their environment. This can be modeled by a three-spin system with two different dipolar couplings D and D' as depicted in Fig. 1b. In an extension of the model discussed above, we undertake to find the spin-diffusion rate in this system analytically. The Hamiltonian $H = H_Z + H_D^{12} + H_D^{13}$ with three independent chemical shifts $\omega_1, \omega_2, \omega_3$ and two dipolar couplings D and D' is straightforward. The dipolar coupling H_D^{23} between the exchanging nuclei is not relevant. The full Liouville space of this system has dimension 64 and the relevant subspace where spin dynamics happens starting from any initial condition $\rho(0)$ with an arbitrary amount of polarization on each nucleus,

$$\rho(0) = x\mathbf{S}_{1z} + y\mathbf{S}_{2z} + z\mathbf{S}_{3z}, \quad [11]$$

has still dimension 16, disregarding the constant of the motion $\mathbf{S}_{1z} + \mathbf{S}_{2z} + \mathbf{S}_{3z}$. An appropriate basis \mathbf{O}_i of this subspace and the commutators of this basis with the different parts of the Hamiltonian are given in the Appendix. Spin dynamics is described by the Liouville equation plus an exchange contribution represented by the permutation operator \mathbf{P}_{23} for nuclei 2 and 3. Thus, the full equation of motion is

$$\dot{\rho} = -i[H, \rho] + k(\mathbf{P}_{23} - \mathbf{1})\rho. \quad [12]$$

The action of \mathbf{P}_{23} on the basis operators \mathbf{O}_i is trivial because it reduces to the permutation of the indices 2 and 3. Using the commutators in the Appendix and the definition of \mathbf{P}_{23} , the equation of motion can again be transformed to a linear differential equation for the coefficients of the \mathbf{O}_i with a matrix that we spare the reader.

We begin the calculation of the spin-diffusion rate in this system by noting that $\rho(0)$ is a linear combination of $\mathbf{S}_{1z} + \mathbf{S}_{2z} + \mathbf{S}_{3z}$, $\mathbf{O}_1 = \frac{1}{\sqrt{3}}(2\mathbf{S}_{1z} - \mathbf{S}_{2z} - \mathbf{S}_{3z})$, and $\mathbf{O}_4 = \mathbf{S}_{3z} - \mathbf{S}_{2z}$ for all values of the coefficients x, y , and z . All these terms are conserved under the Zeeman interaction, but they differ in their behavior under the dipolar interaction and the exchange. The overall polarization $\mathbf{S}_{1z} + \mathbf{S}_{2z} + \mathbf{S}_{3z}$ is conserved under both of them, whereas \mathbf{O}_4 decays under the influence of the exchange. This is expressed by the term $k(P_{23} - 1)\mathbf{O}_4 = -2k\mathbf{O}_4$ in Eq. [12] that leads to an exponentially decaying expectation value $\langle \mathbf{O}_4 \rangle$, the rate of decay being $2k$. \mathbf{O}_1 , on the other hand, is conserved by the exchange, because $k(P_{23} - 1)\mathbf{O}_1 = 0$. Only the combined action of the exchange and the dipolar couplings makes the expectation value of \mathbf{O}_1 decay slowly. This decay is the spin-diffusion process we are interested in.

For vanishing dipolar couplings, \mathbf{O}_1 is an eigenvector with eigenvalue 0. For nonvanishing dipolar couplings, we again expand this eigenvalue λ as a power series of D and D' that is inserted into the characteristic polynomial of the system. By setting this polynomial equal to zero, we find by computer algebra

$$\lambda = -\frac{3}{4} \frac{(D\Delta_{13} - D'\Delta_{12})^2 k}{\Delta_{12}^2 \Delta_{13}^2 + k^2 (\Delta_{12} + \Delta_{13})^2} + O(\|D, D'\|^3), \quad [13]$$

where $\Delta_{ij} = \omega_i - \omega_j$. Note that Eq. [13] predicts $\lambda = 0$ for $D/D' = \Delta_{12}/\Delta_{13}$ which implies that spin diffusion is suppressed for this special situation. This statement is true even if the cubic terms in D, D' are included in Eq. [13]. If, however, $\Delta_{13} \gg \Delta_{12}$ and D and D' are of similar size, Eq. [13] reduces to

$$\lambda = -\frac{3}{4} \frac{D^2 k}{\Delta_{12}^2 + k^2} \left(1 + O\left(\frac{\Delta_{12}}{\Delta_{13}}\right)^2 \right) + O(\|D, D'\|^3). \quad [14]$$

Equation [14] says that only the dipolar coupling of the pair of nuclei with the smaller of the chemical-shift differences is relevant, as we have intuitively argued in (3). It can also be seen that the result is the same as in the two-spin model discussed above except for a factor of $\frac{3}{2}$ by which the spin-diffusion rate is enhanced in the more realistic model. The simplified model is thus nicely confirmed as a valuable tool for calculations of this kind. In the next section, we shall use it for the more involved case of spin $S = 1$ nuclei.

Spins $S = 1$. In this section, we consider a dipolar-coupled system of two nuclei with spins $S = 1$ that also experience, in addition to the Zeeman interaction with the static

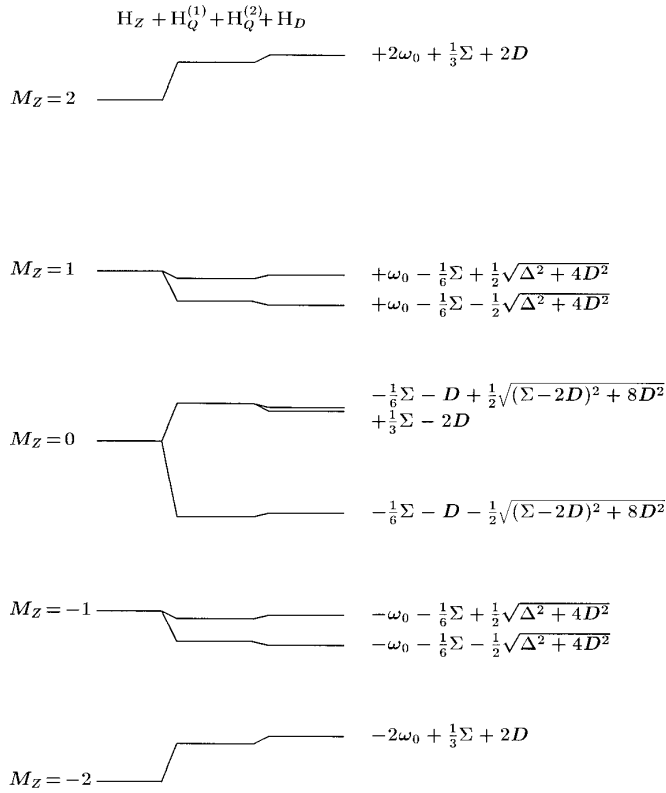


FIG. 2. Energy level diagram of two spins $S = 1$ including a common Zeeman interaction, individual quadrupole interactions, and a weak dipolar interaction. There are zero-quantum transitions ($\Delta M = 0$) in the $M_Z = 0$ and $M_Z = \pm 1$ Zeeman levels. The quadrupole splitting of the $M_Z = \pm 1$ Zeeman levels is given by the difference Δ of the individual quadrupole interactions, whereas the splitting of the $M_Z = 0$ Zeeman level is given by their sum Σ .

magnetic field, a quadrupolar interaction with the local electric-field gradients. The high-field Hamiltonian in the rotating frame is

$$\begin{aligned} H &= H_Q + H_D \\ &= \omega_{Q,1}(\mathbf{S}_{1z}^2 - \frac{2}{3}\mathbf{1}) + \omega_{Q,2}(\mathbf{S}_{2z}^2 - \frac{2}{3}\mathbf{1}) \\ &\quad + D\{2\mathbf{S}_{1z}\mathbf{S}_{2z} - \frac{1}{2}(\mathbf{S}_{1+}\mathbf{S}_{2-} + \mathbf{S}_{1-}\mathbf{S}_{2+})\}, \quad [15] \end{aligned}$$

where $\omega_{Q,1}$ and $\omega_{Q,2}$ are the quadrupolar frequencies of nuclei 1 and 2 and D is again the dipolar coupling strength (δ). Diagonalization of this Hamiltonian ($I0$) leads to the energy level diagram of Fig. 2. From the commutation relation $[H_Z, H_D] = 0$, it is clear that spin dynamics induced by the dipolar coupling is limited to $\Delta M = 0$ transitions. Inspection of Fig. 2 shows several such zero-quantum transitions within the $M_Z = \pm 1$ and $M_Z = 0$ Zeeman levels which are relevant for spin diffusion (2).

Spins with $S = 1$ permit two kinds of spin order, namely Zeeman order or polarization described by \mathbf{S}_z , and quadrupolar

order, also named alignment, described by $(\mathbf{S}_z^2 - \frac{2}{3}\mathbf{1})$. First, we consider the case where both nuclei carry different amounts of Zeeman order. Invoking the same arguments as we did for spins $S = \frac{1}{2}$, we can restrict ourselves to the special case

$$\rho(0) = \mathbf{S}_{1z} - \mathbf{S}_{2z}. \quad [16]$$

Starting from this state, the density matrix evolves under the influence of the Hamiltonian [15] in a 7-dimensional subspace of the full Liouville space. A possible basis of this subspace is

$$\begin{aligned} \mathbf{O}_1 &= \mathbf{S}_{1z} - \mathbf{S}_{2z}, & \mathbf{O}_2 &= \mathbf{S}_{1+}\mathbf{S}_{2-} - \mathbf{S}_{1-}\mathbf{S}_{2+}, \\ \mathbf{O}_3 &= \mathbf{S}_{1z}(\mathbf{S}_{1+}\mathbf{S}_{2-} + \mathbf{S}_{1-}\mathbf{S}_{2+}), & \mathbf{O}_4 &= (\mathbf{S}_{1+}\mathbf{S}_{2-} + \mathbf{S}_{1-}\mathbf{S}_{2+})\mathbf{S}_{2z}, \\ \mathbf{O}_5 &= (\mathbf{S}_{1z}\mathbf{S}_{2z} + \frac{2}{3}\mathbf{1})\mathbf{O}_1, & \mathbf{O}_6 &= \mathbf{S}_{1z}\mathbf{O}_2\mathbf{S}_{2z}, \\ \mathbf{O}_7 &= \mathbf{S}_{1+}^2\mathbf{S}_{2-}^2 - \mathbf{S}_{1-}^2\mathbf{S}_{2+}^2. \end{aligned} \quad [17]$$

This choice of basis is convenient for a start, but shortly it will turn out that it is in no way optimal. The relevant polarization difference \mathbf{O}_1 is orthogonal to all other basis operators which are, however, not orthogonal among themselves. The commutators of the quadrupolar part of the Hamiltonian with the basis operators are

$$\begin{aligned} [H_Q, \mathbf{O}_1] &= 0 \\ [H_Q, \mathbf{O}_2] &= -\Delta\mathbf{O}_2 + (\Sigma + \Delta)\mathbf{O}_3 + (\Delta - \Sigma)\mathbf{O}_4 \\ [H_Q, \mathbf{O}_3] &= \Sigma\mathbf{O}_3 + (\Delta - \Sigma)\mathbf{O}_6 \\ [H_Q, \mathbf{O}_4] &= -\Sigma\mathbf{O}_4 + (\Sigma + \Delta)\mathbf{O}_6 \\ [H_Q, \mathbf{O}_5] &= 0 \quad [H_Q, \mathbf{O}_6] = \Delta\mathbf{O}_6 \\ [H_Q, \mathbf{O}_7] &= 0, \end{aligned} \quad [18]$$

where $\Delta = \omega_{Q,1} - \omega_{Q,2}$ and $\Sigma = \omega_{Q,1} + \omega_{Q,2}$. The commutators with the dipolar part of the Hamiltonian are

$$\begin{aligned} [H_D, \mathbf{O}_1] &= \mathbf{O}_2 \\ [H_D, \mathbf{O}_2] &= \frac{8}{3}\mathbf{O}_1 - 2\mathbf{O}_3 + 2\mathbf{O}_4 + 2\mathbf{O}_5 \\ [H_D, \mathbf{O}_3] &= \frac{4}{3}\mathbf{O}_1 - 2\mathbf{O}_3 + \mathbf{O}_5 + 2\mathbf{O}_6 + \frac{1}{2}\mathbf{O}_7 \\ [H_D, \mathbf{O}_4] &= \frac{4}{3}\mathbf{O}_1 + 2\mathbf{O}_4 + \mathbf{O}_5 - 2\mathbf{O}_6 - \frac{1}{2}\mathbf{O}_7 \\ [H_D, \mathbf{O}_5] &= \frac{2}{3}\mathbf{O}_2 - \mathbf{O}_3 - \mathbf{O}_4 + 2\mathbf{O}_6 \\ [H_D, \mathbf{O}_6] &= \frac{2}{3}\mathbf{O}_1 + 2\mathbf{O}_5 \\ [H_D, \mathbf{O}_7] &= 2\mathbf{O}_3 - 2\mathbf{O}_4, \end{aligned} \quad [19]$$

where the common factor D has been dropped on all right-hand sides. Using these relations we are led to a linear differ-

ential equation for the expansion coefficients of $\boldsymbol{\rho}(t)$ as in the previous examples. The system matrix \mathbf{A} is neither symmetric nor very informative. However, after the basis transformation

$$\begin{aligned}\mathbf{O}'_1 &= \frac{1}{3}\mathbf{O}_1 + \mathbf{O}_5, & \mathbf{O}'_2 &= \frac{1}{2}(\mathbf{O}_2 - \mathbf{O}_3 - \mathbf{O}_4) + \mathbf{O}_6, \\ \mathbf{O}'_3 &= -\frac{1}{2}(\mathbf{O}_2 - \mathbf{O}_3 - \mathbf{O}_4), & \mathbf{O}'_4 &= \mathbf{O}_4 - \mathbf{O}_6, \\ \mathbf{O}'_5 &= \mathbf{O}_3 - \mathbf{O}_6, & \mathbf{O}'_6 &= \frac{2}{3}\mathbf{O}_1 - \mathbf{O}_5, \\ \mathbf{O}'_7 &= \frac{1}{2}\mathbf{O}_7,\end{aligned}\quad [20]$$

we find the skew-hermitian ($\mathbf{A}^\dagger = -\mathbf{A}$) and block-diagonal system matrix

$$\mathbf{A}' = -i \begin{bmatrix} 0 & 2D & 0 & & & & \\ 2D & 0 & \Delta & & & & \\ 0 & \Delta & 0 & & & & \\ & & & -\Sigma' & 0 & D & -D \\ & & & 0 & \Sigma' & D & D \\ & & & D & D & 0 & 0 \\ & & & -D & D & 0 & 0 \end{bmatrix}, \quad [21]$$

where $\Sigma' = \omega_{Q,1} + \omega_{Q,2} - 2D = \Sigma - 2D$ and $\Delta = \omega_{Q,1} - \omega_{Q,2}$. The two blocks have a simple physical interpretation. The 3×3 block is equivalent to a system of two spins $S = \frac{1}{2}$ with a doubled dipolar coupling (see Eq. [6]). It describes the spin dynamics within the $M_z = \pm 1$ Zeeman levels

$$\mathbf{A} = \begin{bmatrix} i\Sigma' - k & 0 & -iD & iD & & & & \\ 0 & -i\Sigma' - k & -iD & -iD & & & & \\ -iD & -iD & -k & 0 & & & & \\ iD & -iD & 0 & -k & & & & \\ k & & & & & & & \\ & k & & & & & & \\ & & k & & & & & \\ & & & k & & & & \\ & & & & k & & & \\ & & & & & k & & \\ & & & & & & k & \\ & & & & & & & k \end{bmatrix}. \quad [23]$$

of Fig. 2. The 4×4 block describes the spin dynamics within the $M_z = 0$ Zeeman level. A different presentation of this decomposition can be found in (2). The basis transformation given in Eq. [20] tells us that the relevant polarization difference \mathbf{O}_1 lives in the 3×3 block with $\frac{1}{3}$ and in the 4×4 block with $\frac{2}{3}$ of its overall expectation value. Suter *et al.* have shown that proton-driven spin diffusion becomes fast in the 3×3 block when Δ is small, and in the 4×4 block when Σ is small. This means that, regardless of the relative signs of $\omega_{Q,1}$ and $\omega_{Q,2}$, spin diffusion becomes fast whenever in the spectrum the resonance lines of the two spins come close to each other.

Our aim is to deduce an expression for motionally driven spin diffusion. For this purpose, we return to the model of a fluctuating interaction strength in a two-spin system. In this model, the quadrupolar coupling of the second nucleus is erratically switched between the values $\omega_{Q,2}$ and $\omega_{Q,2}^*$ at a rate k . Equivalently speaking, the frequency difference is switched from Δ to Δ^* and the sum from Σ to Σ^* . The general situation is quite involved. Therefore, we consider a specific situation where the frequencies $\omega_{Q,1}$, $\omega_{Q,2}$, $\omega_{Q,2}^*$, are related as follows $|\omega_{Q,1}| - |\omega_{Q,2}| \ll |\omega_{Q,1}|$, $|\omega_{Q,2}|$, $|\omega_{Q,1}| - |\omega_{Q,2}^*|$, $|\omega_{Q,2}| - |\omega_{Q,2}^*|$. This situation is shown schematically in Fig. 3a. It includes the two cases of prime interest $\omega_{Q,1} \approx \omega_{Q,2}$ and $\omega_{Q,1} \approx -\omega_{Q,2}$. As mentioned before, spin diffusion proceeds in the first case in the 3×3 block and affects $\frac{1}{3}$ of the polarization difference. The description is the same as in Eq. [7] and yields the result of Eq. [10] with D^2 replaced by $4D^2$. Therefore, the spin-diffusion rate is in the case $\omega_{Q,1} \approx \omega_{Q,2}$

$$\frac{1}{T_{SD}^Z} = \frac{1}{3} \frac{2D^2 k}{\Delta^2 + k^2}. \quad [22]$$

The index Z indicates that this expression applies to the diffusion of Zeeman order or polarization. In the second case of interest, $\omega_{Q,1} \approx -\omega_{Q,2}$, spin diffusion exclusively happens in the 4×4 block and affects $\frac{2}{3}$ of the polarization difference. The description is analogous to that of the former case and leads to the matrix

The relevant eigenvalue close to zero is

$$\begin{aligned}\lambda &= \frac{-k(\Sigma - \Sigma^*)^2 - i\sqrt{(\Sigma + \Sigma^*)^2(4k^2 + \Sigma\Sigma^*)^2}}{\Sigma^2\Sigma^{*2} + k^2(\Sigma + \Sigma^*)^2} \\ &\times D^2 + O(D^4).\end{aligned}\quad [24]$$

The imaginary part of this eigenvalue reflects the fact that the isolated 4×4 block has no constant of the motion which means that the full initial polarization difference oscillates (very slowly) between negative and positive values. This oscillation is not interesting for the matter of spin diffusion,

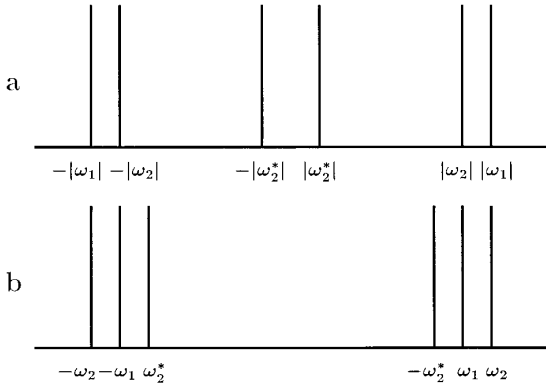


FIG. 3. Frequency relations of three spins $S = 1$ with individual quadrupole interactions. (a) A situation where one frequency difference is much smaller than all others; the spin-diffusion problem has a simple solution. (b) A case where spin diffusion becomes more difficult to treat, and for quadrupolar order even degenerates into cross relaxation.

and in a real system, it will usually be suppressed by additional broadening effects. The spin-diffusion rate caused by the motional driving is given by $\frac{2}{3}$ times the real part of this eigenvalue and for $\Sigma^* \gg \Sigma$ simplifies to

$$\frac{1}{T_{\text{SD}}^Z} = \frac{2}{3} \frac{D^2 k}{\Sigma^2 + k^2}. \quad [25]$$

Thus, we find that *motioally driven* spin diffusion of Zeeman order is independent of the relative signs of $\omega_{Q,1}$ and $\omega_{Q,2}$, as is *proton-driven* spin diffusion (2). Except for a scaling factor on the order of one, the spin-diffusion rate can be obtained formally from Suter's results (2) by replacing the relaxation rate $1/T_{\text{SD}}^Z$ of the zero-quantum coherence by the exchange rate k as we have intuitively argued in (3). The exact value of the scaling factor is model dependent as can be seen from a comparison of the two-spin and three-spin models for spin $S = \frac{1}{2}$ nuclei discussed in the previous section.

The other possible spin order in an $S = 1$ system is quadrupolar order. In a typical exchange experiment with storage of this order, the mixing period starts with

$$\rho(0) = x \left(\mathbf{S}_{1z}^2 - \frac{2}{3} \mathbf{1} \right) + y \left(\mathbf{S}_{2z}^2 - \frac{2}{3} \mathbf{1} \right), \quad [26]$$

where x and y may have arbitrary values. Under the influence of the Hamiltonian of Eq. [15], the density matrix evolves again in a 7-dimensional subspace of the full Liouville space. A suitable basis for this subspace is

$$\begin{aligned} \mathbf{O}_1 &= (\mathbf{S}_{1z}^2 - \frac{2}{3} \mathbf{1}) + (\mathbf{S}_{2z}^2 - \frac{2}{3} \mathbf{1}) \\ \mathbf{O}_2 &= \frac{1}{2} \{ \mathbf{S}_{1z} (\mathbf{S}_{1+} \mathbf{S}_{2-} - \mathbf{S}_{1-} \mathbf{S}_{2+}) - (\mathbf{S}_{1+} \mathbf{S}_{2-} - \mathbf{S}_{1-} \mathbf{S}_{2+}) \mathbf{S}_{2z} \} \\ \mathbf{O}_3 &= -\frac{1}{2} \{ \mathbf{S}_{1z} (\mathbf{S}_{1+} \mathbf{S}_{2-} - \mathbf{S}_{1-} \mathbf{S}_{2+}) \\ &\quad + (\mathbf{S}_{1+} \mathbf{S}_{2-} - \mathbf{S}_{1-} \mathbf{S}_{2+}) \mathbf{S}_{2z} \} \\ &\quad - \mathbf{S}_{1z} (\mathbf{S}_{1+} \mathbf{S}_{2-} + \mathbf{S}_{1-} \mathbf{S}_{2+}) \mathbf{S}_{2z} \\ \mathbf{O}_4 &= \frac{1}{2} (\mathbf{S}_{1+}^2 \mathbf{S}_{2-}^2 + \mathbf{S}_{1-}^2 \mathbf{S}_{2+}^2) - \mathbf{S}_{1z} \mathbf{S}_{2z} \\ &\quad - 3 (\mathbf{S}_{1z}^2 - \frac{2}{3} \mathbf{1}) (\mathbf{S}_{2z}^2 - \frac{2}{3} \mathbf{1}) \\ \mathbf{O}_5 &= \mathbf{S}_{1z}^2 - \mathbf{S}_{2z}^2 \\ \mathbf{O}_6 &= \frac{1}{2} \{ \mathbf{S}_{1z} (\mathbf{S}_{1+} \mathbf{S}_{2-} - \mathbf{S}_{1-} \mathbf{S}_{2+}) + (\mathbf{S}_{1+} \mathbf{S}_{2-} - \mathbf{S}_{1-} \mathbf{S}_{2+}) \mathbf{S}_{2z} \\ &\quad - (\mathbf{S}_{1+} \mathbf{S}_{2-} + \mathbf{S}_{1-} \mathbf{S}_{2+}) \} \\ \mathbf{O}_7 &= \mathbf{S}_{1z} (\mathbf{S}_{1+} \mathbf{S}_{2-} + \mathbf{S}_{1-} \mathbf{S}_{2+}) \mathbf{S}_{2z} \\ &\quad - \frac{1}{2} \{ \mathbf{S}_{1z} (\mathbf{S}_{1+} \mathbf{S}_{2-} - \mathbf{S}_{1-} \mathbf{S}_{2+}) \\ &\quad - (\mathbf{S}_{1+} \mathbf{S}_{2-} - \mathbf{S}_{1-} \mathbf{S}_{2+}) \mathbf{S}_{2z} \} \\ &\quad + \frac{1}{2} (\mathbf{S}_{1+} \mathbf{S}_{2-} + \mathbf{S}_{1-} \mathbf{S}_{2+}), \end{aligned} \quad [27]$$

because it leads to a Liouvillian \mathbf{A} which immediately appears in the block structure already found for Zeeman order in Eq. [21],

$$\mathbf{A} = -i \begin{bmatrix} 0 & 2D & 0 & 0 \\ 2D & 0 & \Sigma' & 2D \\ 0 & \Sigma' & 0 & 0 \\ 0 & 2D & 0 & 0 \\ & & & 0 & 2D & 0 \\ & & & 2D & 0 & \Delta \\ & & & 0 & \Delta & 0 \end{bmatrix}. \quad [28]$$

The decisive difference to Zeeman order is that the sum of quadrupolar spin orders, i.e., \mathbf{O}_1 , is not a constant of the motion, but evolves in the 4×4 block of the matrix and thus in the $M_Z = 0$ Zeeman levels of Fig. 2. Therefore, it may decay and lead to new features of spin diffusion (2). The difference of quadrupolar spin orders, \mathbf{O}_5 , on the other hand, evolves in the 3×3 block. As Suter has pointed out, this implies that quadrupolar order is efficiently transferred whenever $|\omega_{Q,1}| \approx |\omega_{Q,2}|$, with its sign conserved if $\omega_{Q,1} \approx \omega_{Q,2}$, but with its sign reversed if $\omega_{Q,1} \approx -\omega_{Q,2}$.

Motionally driven spin diffusion of quadrupolar order in the 3×3 block of the matrix [28] shows the same behavior as does that of Zeeman order. Because the full expectation value of the relevant operator, \mathbf{O}_5 , now decays in this block, there is no factor of $\frac{1}{3}$ and the spin-diffusion rate of quadrupolar order is three times faster than that of Zeeman order. For $\Delta^* \gg \Delta$, we find

$$\frac{1}{T_{\text{SD}}^{\text{Q}\Delta}} = \frac{2D^2 k}{\Delta^2 + k^2} = g(\Delta) 4D^2. \quad [29]$$

The superscript $Q\Delta$ reminds us that this is the decay rate of the difference of the quadrupolar orders of the two spins, which is the rate at which quadrupolar order is transferred from one spin to the other with its sign conserved. The formula shows that this rate becomes fast when $\omega_{Q,1} \approx \omega_{Q,2}$. Note that this equation coincides with Eq. [10] if the factor 4 introduced by the doubling of the effective dipolar coupling is disregarded. This is because the lineshape factor $g(\Delta)$ in both cases stems from the same exchange process.

The 4×4 block can be treated in analogy to Eq. [23]. The treatment is, however, somewhat more involved because the resulting matrix has not only one eigenvalue λ close to zero but another one that is exactly zero. An inspection of the corresponding eigenvectors shows that in the limit $D \ll \Sigma$ one-half of the expectation value of \mathbf{O}_1 is conserved and the second half decays with a rate $-\lambda$. Therefore, in an ‘‘initial slope’’ view, the spin diffusion rate is $-\lambda/2$. Not very surprisingly, we find in the limit $\Sigma^* \gg \Sigma$

$$\frac{1}{T_{SD}^{Q\Sigma}} = \frac{2D^2k}{\Sigma^2 + k^2} = g(\Sigma)4D^2. \quad [30]$$

Here the superscript $Q\Sigma$ indicates that the formula gives the decay rate of the sum of the quadrupolar orders of the two spins, i.e., the rate at which quadrupolar order is transferred from one spin to the other with its sign reversed. This rate becomes fast when $\omega_{Q,1} \approx -\omega_{Q,2}$.

We conclude that all spin-diffusion rates are independent of the relative sign of the quadrupolar couplings involved and that motionally driven spin diffusion is three times faster for quadrupolar order than for Zeeman order. This theoretical factor of 3 was also derived for proton-driven spin diffusion (2). It is, in fact, independent of the actual driving process considered.

The results obtained so far apply to the frequency relations in Fig. 3a because the relations $\Delta^*, \Sigma^*, \Sigma \gg \Delta \gg D$ or $\Delta^*, \Sigma^*, \Delta \gg \Sigma \gg D$ were assumed to hold, and spin diffusion is therefore limited to either the 3×3 or the 4×4 block of the relevant matrices in Eqs. [21] and [28]. We can easily conceive a situation where spin diffusion appears simultaneously in both blocks. An example is given in Fig. 3b. In such a situation, spin diffusion of Zeeman order gets faster by up to a factor of 2. Quadrupolar order, however, is no longer transferred between the spins but decays for both of them as the result of a cross-relaxation process. The general features of this cross-relaxation process will be discussed later in this article. The experimental system dealt with in the next section fits Fig. 3a, and therefore the theory developed so far should be and, as we shall see, is fully applicable.

Experimental System: Biphenyl

The biphenyl molecule is shown in Fig. 4 together with a single-crystal deuteron NMR spectrum. The spectrum was

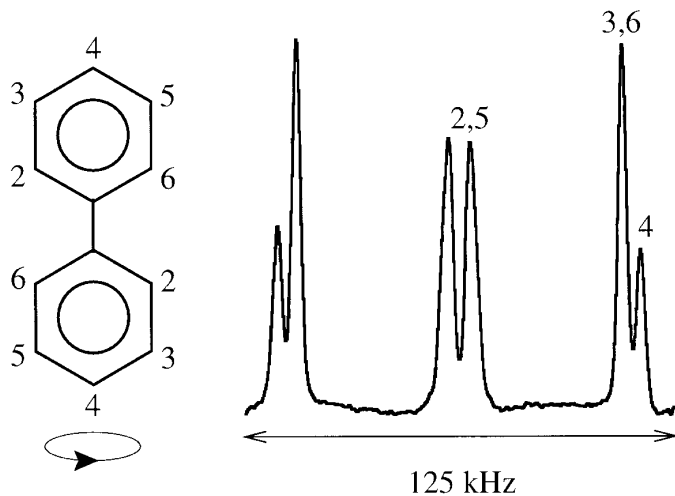


FIG. 4. The biphenyl molecule and its hydrogen sites. The phenyl rings undergo 180° flips about the long molecular axis and thus the hydrogens 3, 4, 5 locally form an experimental realization of the model in Fig. 1b with spins $S = 1$. For an appropriate crystal orientation, the spectrum corresponds to the frequency relations of Fig. 3a, see text.

obtained from a crystal oriented such that the magnetic field \mathbf{B}_0 was in the monoclinic plane. The assignment of the line pairs to the different deuteron sites is indicated by the labeling of the deuterons. The symmetry relations that reduce the spectrum to three pairs of lines have been given in (3).

In the crystal, the molecules undergo thermally activated 180° flips about their long axes (3, 15). This flip process exchanges deuteron 3 with deuteron 5 and deuteron 2 with deuteron 6, but leaves the para deuteron 4 unaffected. Thus, the para deuteron and its neighborhood is a close realization of the model of Fig. 1b. The fact that a given para deuteron has dipolar couplings not only to the deuterons 2 and 5 (and 3 and 6) of its ‘‘own’’ molecule, but to other inversion-symmetry and translation-symmetry equivalent deuterons as well, makes the quantification of the model parameter D (dipolar coupling strength) somewhat ambiguous (3). Therefore, we do not attempt to determine D from the structure of biphenyl and restrict ourselves to noting that dipolar couplings of neighboring deuterons in organic solids are usually in the range of a few hundred radians per second. In 1D and 2D exchange experiments, a polarization transfer from (and to) deuteron 4 to (and from) deuterons 2, 3, 5, and 6 can be observed (3). This polarization transfer occurs on a time scale of $1 \cdot \cdot \cdot 10$ s, and we remind the reader that this is exactly the spin-diffusion process treated in the previous section.

An interpretation of the observed polarization transfer by a chemical-exchange process is evidently out of the question: it would require a breaking and reforming of covalent bonds. That the observed polarization transfer is caused by spin diffusion can be confirmed by a measurement of the transfer

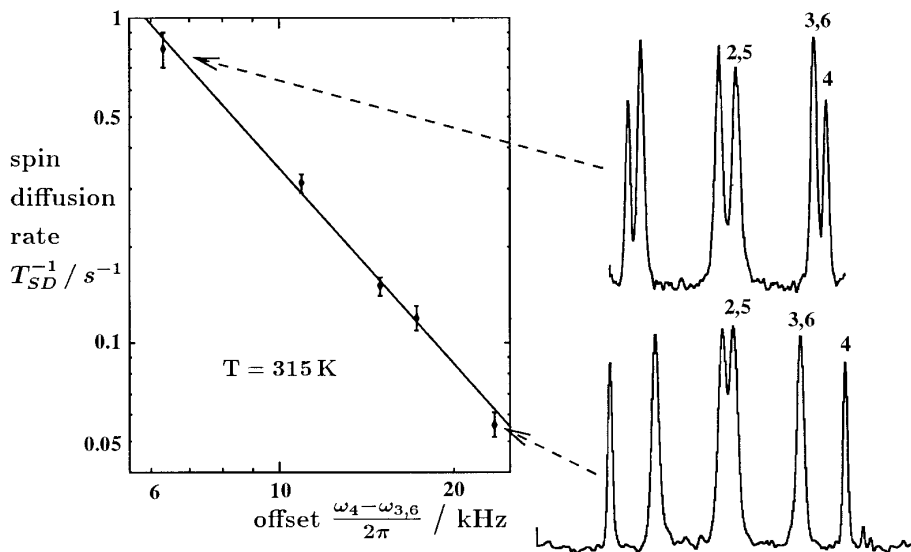


FIG. 5. The offset dependence of the exchange rate between line 4 and line 3, 6 and two spectra for slightly different crystal orientations. This offset dependence rules out a chemical exchange and fits the model of spin diffusion driven by the 180° -flip process.

rate as a function of the spectral line separation. A convenient, direct, and time-saving method of measuring the transfer rate has been described in (3, 13). In the spectrum of Fig. 4, the resonance lines 4 and 3, 6 are closely spaced. Because we know the crystal orientation and have previously measured the deuteron quadrupole coupling tensors in biphenyl (14), we can tell that the quadrupole splittings $2\omega_{Q,3,6}$ and $2\omega_{Q,4}$ have equal signs in Fig. 4. This means that $\Delta = \omega_{Q,3,6} - \omega_{Q,4} = 2\pi \times 6.2$ kHz and that the frequency relations in this spectrum correspond to those of Fig. 3a. Because the flip rate k around and slightly above room temperature is small compared with Δ , we expect from Eq. [22] a $1/\Delta^2$ dependence of the polarization transfer or spin-diffusion rate $1/T_{SD}$. We carried out an experiment at $T = 315$ K, where $k = 3900$ s $^{-1}$. We varied Δ from $2\pi \times 6.2$ to $2\pi \times 23.5$ kHz by rotating the crystal in the applied field, and measured $1/T_{SD}$ by the method described in (3). A rotation angle of no more than 5° was sufficient to scan Δ in the indicated range. This angle is small enough to allow us to neglect any variation of the dipolar coupling strengths in this experiment.

The variation of the spin-diffusion rate $1/T_{SD}^Z$ for Zeeman order together with the spectra corresponding to the end points of the range of Δ scanned in this experiment are shown in Fig. 5. The solid line, which is obviously a good fit to the data, represents a function $const/\Delta^2$. This confirms nicely the predicted Δ dependence of $1/T_{SD}^Z$. At the same time, the data in Fig. 5 support our claim that the observed spin-diffusion process is driven by the molecular 180° -flip process. To further support this statement, we also measured the temperature dependence of the spin-diffusion rate for Zeeman order, $1/T_{SD}^Z$, and that of the quadrupolar order, $1/T_{SD}^Q$, for the crystal orientation that corresponds to the

upper spectrum in Fig. 5 in a larger temperature range than published previously (3). As we shall see presently, this range now includes temperatures where the flip process is frozen out and has become ineffective for driving spin diffusion. In addition, we repeated the measurements of Ermark (15) of the temperature dependence of the rate k of the 180° -flip process by 2D exchange NMR. The results for the temperature dependences of k , $1/T_{SD}^Z$, and $1/T_{SD}^Q$ are plotted in Fig. 6. The solid lines in these plots correspond to the following functions, which are evidently good fits to the measured data,

$$k = 2.3 \times 10^{17} \text{ s}^{-1} \cdot \exp(-E_a/kT)$$

$$\frac{1}{T_{SD}^Q} = 0.023 \text{ s}^{-1} + 1.2 \times 10^{14} \text{ s}^{-1} \cdot \exp(-E_a/kT)$$

$$\frac{1}{T_{SD}^Z} = 0.018 \text{ s}^{-1} + 4.0 \times 10^{13} \text{ s}^{-1} \cdot \exp(-E_a/kT) \quad [31]$$

with $E_a = 83$ kJ mol $^{-1}$. The 180° -flip process obviously follows very well an Arrhenius behavior, whereas the spin-diffusion rates show an additional constant contribution, which has a time constant of close to one minute. This constant contribution is remarkably slow. It is ordinary spin diffusion driven by more or less temperature-independent processes and can be considered to be typical for perdeuterated crystals without significant molecular motions. The temperature-dependent part, on the other hand, shows the same activation energy as the 180° -flip process with the preexponential factor three times larger for quadrupolar order than for Zeeman order. Because $k \ll \Delta$ in the covered temperature

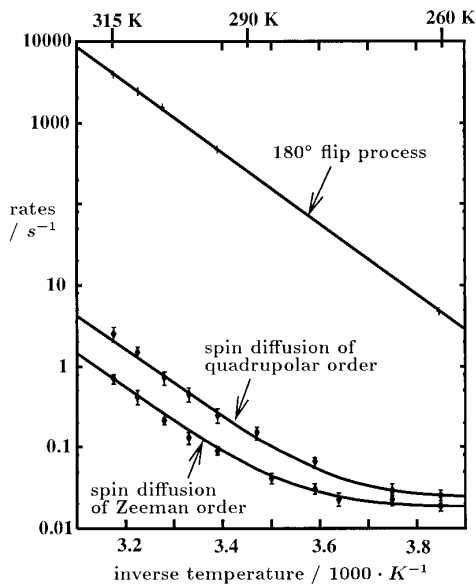


FIG. 6. Temperature dependence of the rate of the 180°-flip process and spin diffusion for a fixed crystal orientation of biphenyl. At the high end of the temperature range, the spin-diffusion rate is proportional to the rate of the driving flip process. At the low end, where the flip process is frozen out, spin diffusion becomes temperature independent and slow. The high-temperature behavior, where spin diffusion is three times faster for quadrupolar than for Zeeman order, is in quantitative agreement with the theoretical prediction.

range, this is in excellent agreement with the theory developed in the previous section. Note that the factor of 3 is lost in the low-temperature range where the flip process is freezing out. In his experiments on malonic acid- d_4 , Suter already observed a factor smaller than 3 (2). Note also that the measured activation energy of the flip process is found to be slightly higher than reported by Ermark (3, 15) but still within the relatively large error limits of those measurements. According to Eqs. [22] and [29], the factor by which the spin-diffusion rates are lower than the rate k of the driving process can be used to calculate the effective dipolar coupling D of deuterons 4 and 3. With $\Delta = 2\pi \times 6.2$ kHz, taken directly from the spectrum, we find $D = 2\pi \times 107$ Hz. This fits well into the expected range of dipolar couplings. Beyond providing a proof for the possibility of motional driving of spin diffusion, these results on biphenyl demonstrate, at the low-temperature end of our measurements, how slow spin diffusion of deuterons can be in favorable cases, and at the high-temperature end, how fast spin diffusion can get without any change in the dipolar coupling strength, if there is an appropriate driving process.

CROSS RELAXATION OF QUADROPOLAR ORDER OF COUPLED SPINS $S = 1$

Connection of Cross Relaxation and Spin Diffusion

As mentioned above, quadrupolar order differs from Zeeman order in that the sum of the quadrupolar orders of two

spins $S = 1$ is not conserved under dipolar coupling. The smaller $\Sigma = \omega_{Q1} + \omega_{Q2}$ is, the faster is the decay of the sum of the quadrupolar orders of Eq. [30]. This transfer of quadrupolar order involves an inversion of its sign (2). On the other hand, the difference of quadrupolar orders decays rapidly when $\Delta = \omega_{Q1} - \omega_{Q2}$ is small. These two cases are well separated whenever either $\Delta \ll \Sigma$ or $\Sigma \ll \Delta$. These conditions are equivalent to $|\Delta| \ll |\omega_{Q1}|, |\omega_{Q2}|$ and $|\Sigma| \ll |\omega_{Q1}|, |\omega_{Q2}|$, respectively. If, however, either $\omega_{Q1} = 0$ or $\omega_{Q2} = 0$, we have $|\Sigma| = |\Delta|$. According to Eqs. [29] and [30], the decay rate of the sum of the single-spin quadrupolar orders becomes equal to that of their difference. A decay of the sum and of the difference of the quadrupolar orders with the same rate simply means that the quadrupolar orders of both spins decay independently of each other. This is shown by the following relation for the first nucleus

$$\begin{aligned} 2 \left\langle \mathbf{S}_{1z}^2 - \frac{2}{3} \mathbf{1} \right\rangle_{(t)} &= \langle \mathbf{O}_1 \rangle_{(t)} + \langle \mathbf{O}_5 \rangle_{(t)} \\ &= \langle \mathbf{O}_1 \rangle_{(0)} \exp\left(\frac{-t}{T_{SD}^{Q\Sigma}}\right) \\ &\quad + \langle \mathbf{O}_5 \rangle_{(0)} \exp\left(-\frac{t}{T_{SD}^{Q\Delta}}\right) \\ &= 2 \cdot \left\langle \mathbf{S}_{1z}^2 - \frac{2}{3} \mathbf{1} \right\rangle_{(0)} \exp\left(\frac{-t}{T_{SD}}\right), \quad [32] \end{aligned}$$

for $T_{SD}^{Q\Sigma} = T_{SD}^{Q\Delta} = T_{SD}$. Spectral spin diffusion disappears in this case and is replaced by a pure cross-relaxation phenomenon. In most systems, however, if $\omega_{Q1} = 0$, the second frequency ω_{Q2} will be fairly large so that cross relaxation is quite slow. The special cross-relaxation case $\omega_{Q1} = 0 \approx \omega_{Q2}$ will therefore be rather rare.

An interesting special case appears, however, when the spin pair is made up of two nuclei with equal quadrupolar interactions, $\omega_{Q1} = \omega_{Q2}$. In this case, the difference of quadrupolar orders of both nuclei is completely irrelevant because it can be neither excited nor detected. A decay of their sum, on the other hand, does not correspond to any transfer of spin order because the spectrum consists of only a single pair of lines. In this special case, the decay of the sum of quadrupolar orders looks just like T_{1Q} relaxation, but its true nature is cross relaxation. Therefore, we will call its time constant T_{1Q}^* . Quadrupolar order decays rapidly when $\Sigma = \omega_{Q1} + \omega_{Q2} = 2\omega_Q$ is small, i.e., when the quadrupolar splitting of the one observable pair of lines is small. Because it is just a degenerate case of spin diffusion, the expression for this decay rate is the same as that for the spin-diffusion rate of Eq. [30], that is,

$$\frac{1}{T_{1Q}^*} = \frac{1}{T_{SD}^{O\Sigma}} = g(\Sigma)4D^2 = g(2\omega_Q)4D^2, \quad [33]$$

where $g(\Sigma)$ represents the lineshape of the zero-quantum transition of the $M_Z = 0$ Zeeman level (Fig. 2), taken at the frequency of the quadrupolar splitting. In the case of motional driving (Eq. [30]), this lineshape is Lorentzian, but in general any lineshape is possible. In the next section, we will present a system where the described cross-relaxation process leads to dramatic effects. It will become clear that the lifetime of quadrupolar order in solids often is not determined by genuine relaxation but by cross relaxation. This explains why, in some systems, T_{1Q} is much shorter than the longitudinal relaxation time T_1 .

Experimental System: Durene

Durene, 2,3,5,6-tetramethylbenzene, crystallizes in the space group $P2_1/a$ with two crystallographically equivalent molecules in the unit cell. Each molecule has two magnetically equivalent aromatic hydrogen sites. If only these sites are deuterated, two deuterons on neighboring molecules form a well-isolated pair with an interatomic distance of 2.9 Å. This is shown in Fig. 7. Because their sites are related by an inversion symmetry, the two deuterons of the pair have identical quadrupole interactions, $\omega_{Q,1} = \omega_{Q,2} = \omega_Q$. To observe the lifetime of the quadrupolar order of this pair of deuterons as a function of ω_Q , we prepared durene- d_2 by

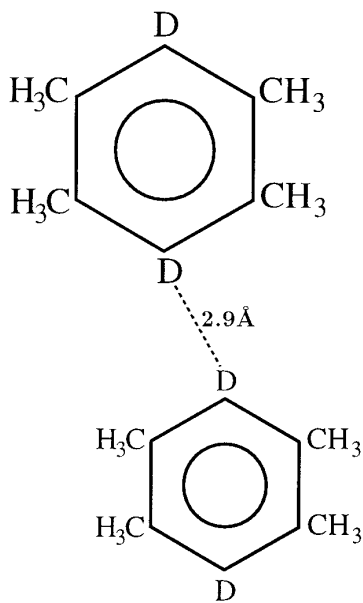


FIG. 7. In solid durene, partially deuterated at the aromatic sites, two neighboring deuterons form a well-isolated and dipolar-coupled pair of equivalent spins $S = 1$. As a consequence, quadrupolar order of these nuclei decays by cross relaxation that is strongly dependent on the quadrupolar splitting.

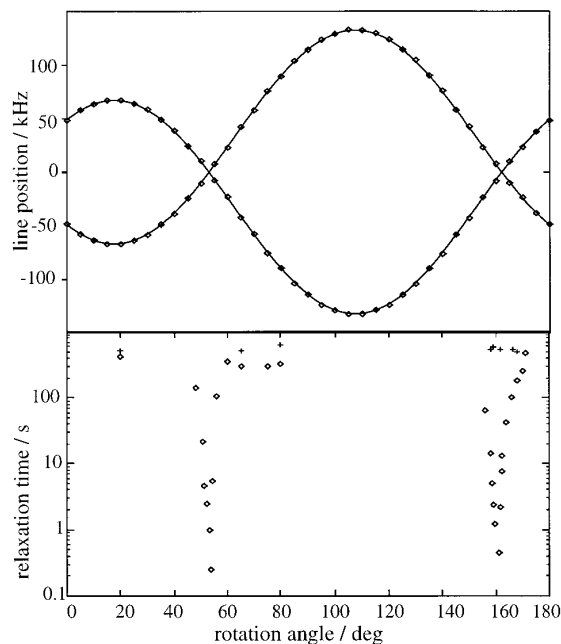


FIG. 8. Rotation pattern of $\omega_Q/2\pi$ of durene- d_2 with the magnetic field in the monoclinic plane, and the corresponding relaxation times T_1 and T_{1Q} . At the points of zero quadrupole splitting, the lifetime of quadrupolar order (\diamond) drops in a resonant way and decouples completely from T_1 (+).

a specific exchange of the aromatic hydrogens of durene in a mixture of CH_3COOD and deuterium bromide (48%) in D_2O . The mixture was stirred at 90°C for three days and the durene was isolated after cooling to room temperature. After a second exchange under identical conditions, the deuteration of the aromatic hydrogens of durene was higher than 98% (according to liquid state ^1H NMR). The durene- d_2 so obtained was recrystallized and purified by extensive zone refining. Crystals of exceptional quality, as judged by the planarity of natural growth planes and lack of visible dislocations, were grown at room temperature by sublimation at 10^{-1} torr in sealed planar glass vessels over several weeks. One of these crystals was prepared as a sample for deuterium NMR. It was oriented such that its monoclinic axis was parallel to the rotation axis of the NMR goniometer. As a consequence, for all rotation angles ϕ the deuterium spectrum of this crystal shows a single resonance split by the quadrupolar interaction. The linewidth of about 1.5 kHz is dominated by the dipolar interaction to the methyl protons. By applying proton decoupling, the linewidth could be reduced to 300–500 Hz, depending on the rotation angle. Using the Jeener–Broekaert pulse sequence (18), together with proton decoupling in the evolution and detection periods, we can create quadrupolar order and monitor its decay even for very small quadrupolar splittings $2\omega_Q$. The rotation pattern of ω_Q is shown in Fig. 8 together with the corresponding lifetime of quadrupolar order, T_{1Q} , and some values of the longitudinal relaxation time T_1 . For most rotation angles, T_1 and T_{1Q} are

on the order of several hundreds of seconds and differ only little. Close to the orientations where the quadrupolar splitting vanishes, however, T_{1Q} drops dramatically by several orders of magnitude, whereas T_1 remains long. This behavior cannot be explained by the standard relaxation theory (5, 16) which is a one-spin theory. The origin of the sharp drops of T_{1Q} is the cross-relaxation process discussed in the previous section as a degenerate case of spin diffusion. The sharp drops of T_{1Q} are thus due to the two-spin character of the system. This claim is further corroborated by the fact that, in one of the respective crystal orientations, we were able to record the well-known (16) multiple-quantum spectrum of the system. This spectrum, which shows the zero-quantum line responsible for cross relaxation, will not be discussed in this article. In Fig. 9, the T_{1Q} values of Fig. 8 are plotted as a function of $\omega_Q/2\pi$. The data are divided into two branches, one for each of the two zero crossings of the quadrupole splitting occurring at $\phi = 53^\circ$ and 162° in the rotation pattern of Fig. 8. The two solid curves of Fig. 9, which evidently are excellent fits to the experimental data, follow the equations

$$\frac{1}{T_{1Q}}(\phi \approx 53^\circ) = 0.0025 \text{ s}^{-1} + 5.7 \left(\frac{1.1 \times 10^7}{\omega_Q^2} + \frac{2 \times 10^{16}}{\omega_Q^4} \right) \text{ s}^{-1},$$

$$\frac{1}{T_{1Q}}(\phi \approx 162^\circ) = 0.0025 \text{ s}^{-1} + \left(\frac{1.1 \times 10^7}{\omega_Q^2} + \frac{2 \times 10^{16}}{\omega_Q^4} \right) \text{ s}^{-1}.$$

[34]

It is clear that these diverging functions can describe $1/T_{1Q}(\omega_Q)$ only as long as ω_Q is large in a sense we are going to state below. It can be seen that the frequency-dependent parts of both curves simply scale with a factor of 5.7. If we make the reasonable assumption that $g(2\omega_Q)$ hardly depends on the crystal orientation, we may conclude from Eq. [33] that this scaling factor must stem from a ratio of $\sqrt{5.7} \approx 2.4$ of the dipolar couplings D for the two orientations. From the structural data for durene (17), the dipolar coupling of the aromatic pair of deuterons can be calculated to be about $2\pi \times 115$ Hz at $\phi = 162^\circ$ and about $2\pi \times 40$ Hz at $\phi = 53^\circ$. The ratio of these two numbers is 2.875 and thus fits reasonably well to the ratio of the decay rates. Equation [33] suggests furthermore that the frequency-dependent parts of Eqs. [34] give the shape $g(2\omega_Q)$ of the zero-quantum line of the coupled deuteron pair. It is dominated by the dipolar coupling to the methyl protons, because during the long (>1 s) mixing period of the Jeener–Broekaert pulse sequence, proton-decoupling was (and had to be) switched off. It can

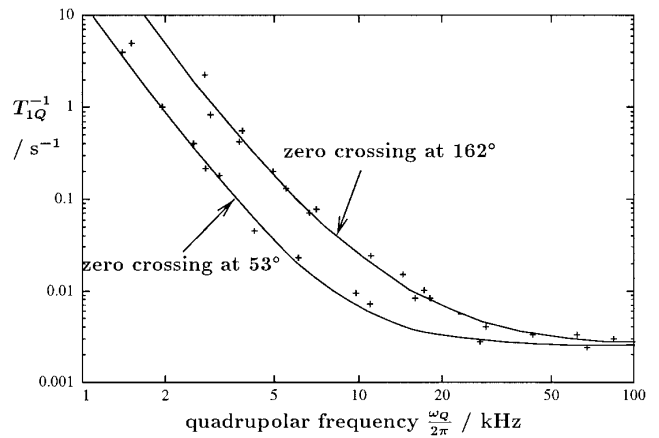


FIG. 9. The lifetime of quadrupolar order in durene vs $\omega_Q/2\pi$. For large $\omega_Q/2\pi$, the lifetime is dominated by genuine relaxation; for $\omega_Q/2\pi$ small, it is dominated by cross relaxation. Each branch corresponds to one zero crossing of ω_Q in the rotation pattern of Fig. 8. The difference of both branches is due to different strengths of the dipolar coupling in the respective crystal orientations.

be seen that $g(2\omega_Q)$ is neither Gaussian nor purely Lorentzian. Only for $\omega_Q > 2\pi \times 5$ kHz, that is, far out in the wings of the line, does the Lorentzian contribution $g(2\omega_Q) = A/[1/\tau^2 + (2\omega_Q)^2] \approx A/(2\omega_Q)^2$ dominate. If it were fully applicable, the inverse quadratic term should be sufficient for ω_Q much larger than $1/\tau$, i.e., at least down to values of ω_Q on the order of the visible linewidth. This is not what we find experimentally. Although the shape of $g(2\omega_Q)$ (neither Lorentzian nor Gaussian nor a mixture thereof) is somewhat surprising, it is not crucial to the nature of the cross-relaxation process described here.

In liquid crystals, T_1 and T_{1Q} are usually considerably shorter than the cross-relaxation time discussed here (5). Thus, cross relaxation can be ignored there. In solids with long T_1 , however, T_{1Q} is often dominated by cross relaxation. It is therefore quite common that T_{1Q} is *much* shorter than T_1 . In the biphenyl spectrum of Fig. 4, for example, where the splitting of the 2, 5 pair of lines is rather small, we observed that the quadrupolar order not only is *transferred* between the various nuclei, but also *decays* on a time scale which is much shorter than T_1 . We further observed in biphenyl that motional driving by the 180° flip makes cross relaxation dependent on temperature in exactly the same way as it makes spin diffusion dependent on temperature.

SUMMARY AND CONCLUSIONS

We have shown experimentally, and elucidated by theoretical models, that spectral spin diffusion can in fact be strongly temperature dependent, if it is motionally driven. To discriminate between spin diffusion and a motional process as the source of an observed polarization transfer, the

measurement of the temperature dependence of the latter is therefore an unsuitable approach. To accomplish this discrimination safely, the dependence of the polarization transfer rate on the spectral difference of the relevant resonances must be checked in a single crystal study as is shown here for the example of biphenyl.

In the theoretical part, we showed that the spin-diffusion problem of three spins with $S = \frac{1}{2}$ as well as that of two coupled spins with $S = 1$ can be treated by explicit construction of the density matrix in a basis of product operators. With the help of computer algebra the corresponding equations can be solved.

In the same formalism, we also described the degeneration of spin diffusion into cross relaxation. In the solid state, this phenomenon affects quadrupolar order rather frequently and becomes evident as a considerable decrease of T_{1Q} compared to T_1 . A comparison of the two time constants, which can be obtained experimentally rather easily, can thus be used to probe the time constant of spin diffusion in the system. If T_{1Q} is much shorter than T_1 , spin diffusion of quadrupolar order may be expected to proceed on the same time scale as T_{1Q} , whereas spin diffusion of Zeeman order will be slower by a factor of 3. If, on the other hand, T_{1Q} is on the order of T_1 for all pairs of lines in a spectrum, the odds are that the spin-diffusion time constants are also on the order of T_1 .

APPENDIX

The three-spin model depicted in Fig. 1b is described in a rather large Liouville space of dimension 64. If at any moment the system is in a state of pure Zeeman polarization according to Eq. [11], however, the spin dynamics is contained in a subspace of dimension 16. The projection of $\rho(0)$ on the constant of the motion $\mathbf{S}_{1z} + \mathbf{S}_{2z} + \mathbf{S}_{3z}$ is conserved and can thus be disregarded. An appropriate orthogonal basis [Trace($\mathbf{O}_i^\dagger \cdot \mathbf{O}_j$) = $4\delta_{ij}$] of the relevant subspace is

$$\begin{aligned} \mathbf{O}_1 &= \frac{1}{\sqrt{3}}(2\mathbf{S}_{1z} - \mathbf{S}_{2z} - \mathbf{S}_{3z}) & \mathbf{O}_2 &= \mathbf{S}_{1+}\mathbf{S}_{2-} - \mathbf{S}_{1-}\mathbf{S}_{2+} \\ \mathbf{O}_3 &= \mathbf{S}_{1+}\mathbf{S}_{2-} + \mathbf{S}_{1-}\mathbf{S}_{2+} & \mathbf{O}_4 &= \mathbf{S}_{3z} - \mathbf{S}_{2z} \\ \mathbf{O}_5 &= \mathbf{S}_{1+}\mathbf{S}_{3-} - \mathbf{S}_{1-}\mathbf{S}_{3+} & \mathbf{O}_6 &= \mathbf{S}_{1+}\mathbf{S}_{3-} - \mathbf{S}_{1-}\mathbf{S}_{3+} \\ \mathbf{O}_7 &= 2 \cdot \mathbf{S}_{2z}\mathbf{O}_6 & \mathbf{O}_8 &= 2 \cdot \mathbf{S}_{2z}\mathbf{O}_5 \\ \mathbf{O}_9 &= \mathbf{S}_{2+}\mathbf{S}_{3-} + \mathbf{S}_{2-}\mathbf{S}_{3+} & \mathbf{O}_{10} &= \mathbf{S}_{2+}\mathbf{S}_{3-} - \mathbf{S}_{2-}\mathbf{S}_{3+} \\ \mathbf{O}_{11} &= 2 \cdot \mathbf{S}_{1z}\mathbf{O}_9 & \mathbf{O}_{12} &= 2 \cdot \mathbf{S}_{1z}\mathbf{O}_{10} \\ \mathbf{O}_{13} &= 2 \cdot \mathbf{S}_{3z}\mathbf{O}_3 & \mathbf{O}_{14} &= 2 \cdot \mathbf{S}_{3z}\mathbf{O}_2 \\ \mathbf{O}_{15} &= 2 \cdot \mathbf{S}_{1z}(\mathbf{S}_{2z} - \mathbf{S}_{3z}) \\ \mathbf{O}_{16} &= \frac{2}{\sqrt{3}}(\mathbf{S}_{1z}\mathbf{S}_{2z} + \mathbf{S}_{1z}\mathbf{S}_{3z} - 2\mathbf{S}_{2z}\mathbf{S}_{3z}). \end{aligned}$$

The transformation of these operators under the permutation operator P_{23} is obvious. Their commutators with the full Zeeman Hamiltonian H_Z are

$$\begin{aligned} [H_Z, \mathbf{O}_1] &= 0 & [H_Z, \mathbf{O}_2] &= \Delta_{12}\mathbf{O}_3 \\ [H_Z, \mathbf{O}_3] &= \Delta_{12}\mathbf{O}_2 & [H_Z, \mathbf{O}_4] &= 0 \\ [H_Z, \mathbf{O}_5] &= \Delta_{13}\mathbf{O}_6 & [H_Z, \mathbf{O}_6] &= \Delta_{13}\mathbf{O}_5 \\ [H_Z, \mathbf{O}_7] &= \Delta_{13}\mathbf{O}_8 & [H_Z, \mathbf{O}_8] &= \Delta_{13}\mathbf{O}_7 \\ [H_Z, \mathbf{O}_9] &= \Delta_{23}\mathbf{O}_{10} & [H_Z, \mathbf{O}_{10}] &= \Delta_{23}\mathbf{O}_9 \\ [H_Z, \mathbf{O}_{11}] &= \Delta_{23}\mathbf{O}_{12} & [H_Z, \mathbf{O}_{12}] &= \Delta_{23}\mathbf{O}_{11} \\ [H_Z, \mathbf{O}_{13}] &= \Delta_{12}\mathbf{O}_{14} & [H_Z, \mathbf{O}_{14}] &= \Delta_{12}\mathbf{O}_{13} \\ [H_Z, \mathbf{O}_{15}] &= [H_Z, \mathbf{O}_{16}] & &= 0, \end{aligned}$$

where $\Delta_{ij} = \omega_i - \omega_j$ is the chemical-shift difference of spins i and j . The commutators with the Hamiltonian of the dipolar coupling of nuclei 1 and 2, H_D^{12} , are

$$\begin{aligned} [H_D^{12}, \mathbf{O}_1] &= \frac{\sqrt{3}}{2}\mathbf{O}_2 & [H_D^{12}, \mathbf{O}_2] &= \frac{\sqrt{3}}{2}\mathbf{O}_1 + \frac{1}{2}\mathbf{O}_4 \\ [H_D^{12}, \mathbf{O}_3] &= 0 & [H_D^{12}, \mathbf{O}_4] &= \frac{1}{2}\mathbf{O}_2 \\ [H_D^{12}, \mathbf{O}_5] &= \mathbf{O}_7 + \frac{1}{2}\mathbf{O}_{11} & [H_D^{12}, \mathbf{O}_6] &= \mathbf{O}_8 + \frac{1}{2}\mathbf{O}_{12} \\ [H_D^{12}, \mathbf{O}_7] &= \mathbf{O}_5 + \frac{1}{2}\mathbf{O}_{10} & [H_D^{12}, \mathbf{O}_8] &= \mathbf{O}_6 + \frac{1}{2}\mathbf{O}_9 \\ [H_D^{12}, \mathbf{O}_9] &= \mathbf{O}_{12} + \frac{1}{2}\mathbf{O}_8 & [H_D^{12}, \mathbf{O}_{10}] &= \mathbf{O}_{11} + \frac{1}{2}\mathbf{O}_7 \\ [H_D^{12}, \mathbf{O}_{11}] &= \mathbf{O}_{10} + \frac{1}{2}\mathbf{O}_5 & [H_D^{12}, \mathbf{O}_{12}] &= \mathbf{O}_9 + \frac{1}{2}\mathbf{O}_6 \\ [H_D^{12}, \mathbf{O}_{13}] &= 0 & [H_D^{12}, \mathbf{O}_{14}] &= \frac{\sqrt{3}}{2}\mathbf{O}_{16} - \frac{1}{2}\mathbf{O}_{15} \\ [H_D^{12}, \mathbf{O}_{15}] &= -\frac{1}{2}\mathbf{O}_{14} & [H_D^{12}, \mathbf{O}_{16}] &= \frac{\sqrt{3}}{2}\mathbf{O}_{14}, \end{aligned}$$

where the common factor of all right-hand sides, the dipolar coupling strength D , was dropped for better readability. From these relations the commutators with the Hamiltonian of the second dipolar coupling, H_D^{13} , can immediately be obtained using the symmetry relation

$$[H_D^{13}, \mathbf{O}_i] = \mathbf{P}_{23}[H_D^{12}, \mathbf{P}_{23}\mathbf{O}_i]. \quad [35]$$

These commutation relations and the action of the permutation operator transform Eq. [12] to a linear differential equation for the expansion coefficients of the density matrix. A power series expansion by computer algebra of the eigenvalue close to zero for small dipolar couplings D and D' leads to the spin-diffusion rate of Eq. [13].

REFERENCES

1. Z. Olender, D. Reichert, A. Müller, H. Zimmermann, R. Poupko, and Z. Luz, *J. Magn. Reson. A* **120**, 31 (1996).
2. D. Suter and R. R. Ernst, *Phys. Rev. B* **32**, 5608 (1985).
3. A. Müller and U. Haeberlen, *Chem. Phys. Lett.* **248**, 249 (1996).
4. B. H. Meier, in "Advances in Magnetic and Optical Resonance" (Warren S. Warren, Ed.), Vol. 18, p. 1, Academic Press, San Diego, 1994.
5. R. R. Vold and R. L. Vold, in "Advances in Magnetic and Optical Resonance" (Warren S. Warren, Ed.), Vol. 16, p. 85, Academic Press, San Diego, 1991.
6. C. P. Slichter, "The Principles of Magnetic Resonance," Springer-Verlag, Berlin, 1980.
7. G. Binsch, *J. Am. Chem. Soc.* **91**, 1304 (1969).
8. Z.-Y. Peng and C. Ho, *J. Magn. Reson.* **82**, 318 (1989).
9. A. Abragam, "The Principles of Nuclear Magnetism," Oxford Univ. Press, London, 1961.
10. C. Müller, S. Idziak, N. Pislewski, and U. Haeberlen, *J. Magn. Reson.* **47**, 227 (1982).
11. J. Trotter, *Acta Crystallogr.* **14**, 1135 (1961).
12. G.-P. Charbonneau and Y. Delugeard, *Acta Crystallogr. Sect. B* **33**, 1586 (1977).
13. N. M. Szeverenyi, A. Bax, and G. E. Maciel, *J. Am. Chem. Soc.* **105**, 2579 (1983).
14. L. von Laue, F. Ermark, A. Gölzhäuser, U. Haeberlen, and U. Häcker, *J. Phys.: Condens. Matter* **8**, 3977 (1996).
15. F. Ermark, Ph.D. Thesis, University of Heidelberg, 1993.
16. R. Poupko, R. L. Vold, and R. R. Vold, *J. Magn. Reson.* **34**, 67 (1979).
17. C. H. Stam, *Acta Crystallogr. Sect. B* **28**, 2630 (1972).
18. J. Jeener und P. Broekaert, *Phys. Rev.* **157**, 232 (1967).